Grand Canonical Monte Carlo Simulation Study of Methane Adsorption at an Open Graphite Surface and in Slitlike Carbon Pores at 273 K

Piotr Kowalczyk,*[,†,‡] Hideki Tanaka,[†] Katsumi Kaneko,[†] Artur P. Terzyk,*[,§] and Duong D. Do[||]

Department of Chemistry, Faculty of Science, Chiba University, 1-3 Yayoi, Chiba, 263, Japan, Department III, Institute of Physical Chemistry, Polish Academy of Science, Kasprzaka Street 44/52, 01-224 Warsaw, Poland, Department of Chemistry, Physicochemistry of Carbon Materials Research Group, N. Copernicus University, Gagarin Street 7, 87-100 Torun, Poland, and Department of Chemical Engineering, University of Queensland, St. Lucia, Queensland 4072, Australia

Received January 17, 2005. In Final Form: March 15, 2005

Grand canonical Monte Carlo (GCMC) simulation was used for the systematic investigation of the supercritical methane adsorption at 273 K on an open graphite surface and in slitlike micropores of different sizes. For both considered adsorption systems the calculated excess adsorption isotherms exhibit a maximum. The effect of the pore size on the maximum surface excess and isosteric enthalpy of adsorption for methane storage at 273 K is discussed. The microscopic detailed picture of methane densification near the homogeneous graphite wall and in slitlike pores at 273 K is presented with selected local density profiles and snapshots. Finally, the reliable pore size distributions, obtained in the range of the microporosity, for two pitch-based microporous activated carbon fibers are calculated from the local excess adsorption isotherms obtained via the GCMC simulation. The current systematic study of supercritical methane adsorption both on an open graphite surface and in slitlike micropores performed by the GCMC summarizes recent investigations performed at slightly different temperatures and usually a lower pressure range by advanced methods based on the statistical thermodynamics.

Introduction

Supercritical adsorption on open surfaces and in highly porous media has been a topic of intense investigations because of the increasing importance of the high-pressure storage of high-value clean energy substances such as methane and hydrogen.[1−5] Recently, many researchers have shown that nanoscience has the potential to provide revolutionary new capabilities that have a profound impact on alternative fuels storage.[3−6] The trend of energy source will shift from conventional fossil fuels to alternative fuels (i.e., primary hydrogen and methane) because of the necessity of protection of the global environment.[7] There are plenty of environmentally harmful substances, among which special restrictions are imposed on carbon monoxide (CO), carbon dioxide (CO_2), total hydrocarbons (THC), nitrogen oxide (NO_x), particulate matter (PM), and soluble organic fraction (SOF). Obviously, methane and hydrogen have received much attention because of the energy and environmental aspects.[4,8−10] As commonly known, methane seems to be the perfect alternative for clean energy because of its low emission of CO_2 and lack of emission of NO_x and sulfur oxide (SO_x) during combustion in comparison to other fuels, for example, coal. Despite its potential as an alternative energy source, methane has a severe greenhouse effect. As a matter of fact its greenhouse effect is more significant than that of CO_2.[11] It is important to keep in mind that there is a large quantity of methane in the ocean, which exists in the form of methane hydrate (i.e., clathrate compound of water and methane molecules).[12] Finally, methane is the major component of natural gas, coal bed gas, and some exhaust gases of petrochemical or chemical units. Unfortunately, handling of methane or hydrogen sources is not easy because of the difficult storage of these species at ambient temperatures.[1,13] These gases are in a supercritical state at room temperatures (i.e., they do not liquefy, for methane the critical temperature is $T_c = 191$ K). Generally speaking, there are three ways to enhance the storage efficiency of natural gas: the liquefied natural gas (LNG), the compressed natural gas (CNG), and the adsorbed natural gas (ANG).[1,14] As we mentioned above, it is impossible to liquefy methane due to its supercritical state at room temperature. Thus, it requires a harsh condition of high pressure and/or low temperature to compress or liquefy. As a result it is difficult to visualize the realization of the LNG in the car technology and so forth. The second

* To whom correspondence should be addressed. E-mail: pkow@pchem2.s.chiba-u.ac.jp (P.K.); aterzyk@chem.uni.torun.pl (A.P.T.).
† Chiba University.
‡ Polish Academy of Science.
§ N. Copernicus University.
|| University of Queensland.

(1) Lozano-Castello, D.; Alcaniz-Monge, J.; de la Casa-Lillo, M. A.; Cazorla-Amoros. D.; Linares-Solano, A. *Fuel* **2002**, *81*, 1777.
(2) Biloe, S.; Goetz, V.; Guillot, A. *Carbon* **2002**, *40*, 1295.
(3) Jiang, S.; Zollweg, J. A.; Gubbins, K. E. *J. Phys. Chem. B* **1994**, *98*, 5709.
(4) Menon, V. C.; Komarneni, S. *J. Porous Mater.* **1998**, *5*, 43.
(5) Eddaoudi, M.; Kim, J.; Rosi, N.; Vodak, D.; Wachter, J.; O'Keeffe, M.; Yaghi, O. M. *Science* **2002**, *295*, 469.
(6) Atwood, J. L.; Barbour, L. J.; Jerga, A. *Science* **2002**, *296*, 2367.
(7) Carslaw, D. C.; Fricker, N. *Chem. Ind.* **1995**, *7*, 601.
(8) Wang, Q.; Johnson, J. K. *J. Chem. Phys.* **1999**, *110*, 577.
(9) Benard, P.; Chahine, R. *Langmuir* **1997**, *13*, 808.
(10) Malbrunot, P.; Vidal, D.; Vermesse, J.; Chahine, R.; Bose, T. *Langmuir* **1992**, *8*, 577.
(11) Murata K. *Fundamental study of high pressure adsorption of supercritical gases*; Chiba University: Chiba, 2001.
(12) Sloan, E. D. *Clathrate hydrates of natural gases*; Marcel Dekker: New York, 1990.
(13) Menon, V. C. *Chem. Rev.* **1968**, *68*, 277.
(14) Murata, K.; El-Merraoui, M.; Kaneko, K. *J. Chem. Phys.* **2000**, *114*, 4196.

10.1021/la050126f CCC: $30.25
Published on Web 04/30/2005

method, that is, CNG, is characterized by extreme conditions (i.e., very high pressure typically more than 150 atm).[1] Moreover, CNG requires a high pressure-resistant cylindrical vessel that is generally difficult to integrate within a limited space. As a result CNG seems to be impractical from the point of cost and safety. The last method, that is, ANG, seems to be very interesting and promising due to the possibility to obtain high storage at normal conditions and relatively low pressure by adoption of highly uniform microporous materials.[15−18] Furthermore, ANG is much safer than CNG. The main key problem connected with ANG is to obtain the high value of the supercritical methane storage.[1,4,19] To obtain the high efficiency of the methane storage a new breed of materials (i.e., superactivated carbons, activated carbon fibers, carbon monoliths, single-walled carbon nanotubes, carbon nanohorns, organic−inorganic hybrid porous complexes) characterized by their high adsorption capacity, hydrophobic nature, and high adsorption/desorption rate are studied. They predominantly consist of micropores of width around 0.8 nm (i.e., greater than the thickness of two methane molecules), high packing density, low heat of adsorption, and high heat capacity to minimize changes in the vessel's temperature during the adsorption/desorption processes.[1,5,6,20−22] The search for a suitable material for the alternative fuels storage is currently an active area of research. New synthesis techniques have opened the door to designing materials with specific architectures to yield desired properties.[5,6,20,23,24] A major advantage of nanostructure materials for alternative fuels storage is that specific architectures can be designed into these materials to enhance the weight percentage of stored fluid and to control the kinetics involved in the adsorption/release of fluid. It is worthwhile to point out that the strength of the molecular binding may be enhanced by adding suitable elements.[21] As pointed out by Matranga et al., grand canonical Monte Carlo (GCMC) simulation can be successfully applied to design the optimal slitlike pore size of carbonaceous materials for methane storage.[25] Similarly, Cao et al.[26] used GCMC simulation to optimize the structure of layer pillared pores. Inomata et al. pointed out that the important parameter of adsorbents is their bulk density.[27] For this reason the main component of the carbonaceous material, that is, single graphite-like crystal, should consist of a relatively small number of stacking planes because they add to the space inaccessible for methane storage.

Fundamental studies of atomic and molecular processes involved in methane adsorption and release are needed to enable the design of improved materials. Theory and computation may be used not only for interpretation of experimental results but also to provide better insight into the adsorption mechanism.[28,29] Proper models of the adsorption system provide a basis for understanding the adsorption behavior and for predicting the type of materials and conditions of efficient adsorption storage. The theoretical treatment of the supercritical or the near-critical region is still not fully understood compared to the subcritical one.[30,31] As a result, there are many key questions that have not been resolved so far. However, several features of supercritical adsorption are well-known from many extensive theoretical studies. At first, under the supercritical conditions the fluids are characterized by weaker adsorption caused by thermal motion and relatively weak fluid−fluid interaction of molecules, for this reason the term "adsorption" under supercritical condition is more appropriately replaced by "densification".[30−32] In fact, adsorption of supercritical fluids is generally monomolecular (it also can occur beyond the first layer if pressure is high enough), and the condensed phase never surrounds the porous medium. Consequently, it is impossible to obtain reliable information about the pore size distribution (PSD) in the range of mesopores, whereas, the analysis of the micropore region should be effective as a result of the lack of disturbances caused by polymolecular adsorption or capillary condensation.[31] Second, adsorption of supercritical fluids when plotted as surface excess of adsorption versus pressure for temperature close to the critical temperature exhibits a maximum at a pressure close to the critical pressure, and especially when the temperature is slightly greater than the critical temperature, the maximum behaves like a very sharp spike.[3,29−31,33−35] It is well documented that the potential energies generated by pore walls, temperature, dimension, and shape of the pore impact on the position and shape of the surface excess maximum.[28,29] However, generally we can suspect that, as the pore size increases, the position of the maxima are shifted to higher bulk densities (i.e., pressures).[29] Next, for the fixed temperature the flattering of the excess adsorption isotherms is expected with increasing pore size.[29] Moreover, as shown by many researchers, the dependence of the maximum excess adsorption on the pore size should be characterized not by the monotonic but rather by the oscillatory behavior due to the packing effect of adsorbed molecules.[28,31] This feature is closely related to the properties of the one-center Lennard-Jones (LJ) model of the fluid−fluid interaction and the model of the pore geometry. The adsorption process under the supercritical condition should be characterized by the layering mechanism; however, as a result of the thermal motion and relatively weak fluid−fluid molecular interaction the low intensity of the second peak, even much lower than the intensity of the third peak, on the local density profile should be expected.[31,36] Besides this, the adsorbed phase density in the central part of the pore (i.e., the core of the pore) should be very close to the bulk phase density upon the pore size increasing. Finally, the understanding of critical phenomena in pores characterized by molecular dimensions is essential for the characterization of micro- and mesoporous solid materials and the development of the proper thermodynamic approaches.

(15) Cracknell, R. F.; Gordon, P.; Gubbins, K. E. *J. Phys. Chem.* **1993**, *97*, 494.
(16) Matsumoto, A.; Kaneko, K. *J. Chem. Soc., Faraday Trans.* **1989**, *85*, 3434.
(17) Wei, S.; Johnson, K. J. *Phys. Rev. Lett.* **2003**, *91*, 015504.
(18) Challa, S. R.; Johnson, K. J. *J. Chem. Phys.* **1999**, *111*, 724.
(19) Aukett, P. N.; Quirke, N.; Riddiford, S.; Tennison, S. R. *Carbon* **1992**, *30*, 913.
(20) Seki, K. *Chem. Commun.* **2001**, 1496.
(21) Hattori, Y.; Konishi, T.; Kaneko, K. *Chem. Phys. Lett.* **2002**, *355*, 37.
(22) Kaneko, K.; Murata, K. *Adsorption* **1997**, *3*, 197.
(23) Li, D.; Kaneko, K. *J. Phys. Chem. B* **2000**, *104*, 8940.
(24) Duren, T.; Snurr, R. Q. *J. Phys. Chem. B* **2004**, *108*, 15703.
(25) Matranga, K. R.; Myers, A. L.; Glandt, D. *Chem. Eng. Sci.* **1992**, *47*, 1569.
(26) Cao, D.; Wang, W.; Duan, X. *J. Colloid Interface Sci.* **2002**, *254*, 1.
(27) Inomata, K.; Kanazawa, K.; Urabe, Y.; Hosono, H.; Araki, T. *Carbon* **2002**, *40*, 87.
(28) McEnaney, B.; Mays, J.; Chen, X. *Fuel* **1998**, *77*, 557.
(29) Tan, Z.; Gubbins, K. E. *J. Phys. Chem. B* **1990**, *94*, 6061.
(30) Do, D. D.; Do, H. D.; Ustinov, E. A. *Langmuir* **2003**, *19*, 2215.
(31) Ustinov, E. A.; Do, D. D. *Langmuir* **2003**, *19*, 8349.
(32) Gusev, V.; O'Brien, J.; Seaton, N. *Langmuir* **1997**, *13*, 2815.
(33) Aranovich, G.; Donohue, M. *J. Colloid Interface Sci.* **1996**, *180*, 537.
(34) Subramanian, R.; Pyada, H.; Lira, C. *Ind. Eng. Chem. Res.* **1995**, *34*, 3830.
(35) Zhou, L.; Zhou, Y.; Li, M.; Chen, P.; Wang, Y. *Langmuir* **2000**, *16*, 5955.
(36) Vermesse, J.; Lesveque, D. *J. Chem. Phys.* **1994**, *101*, 9063.

It is worth pointing out that the critical phenomena of methane in slitlike pores were extensively studied by Vishnyakov et al.[37] and Jiang et al.[38] In the mentioned papers the authors applied advanced methods of confined fluid modeling to study the shifting of the critical parameters due to presence of the strong solid−fluid interactions. Similarly, Gusev et al.[32] investigated the ability of pore size analysis of BPL-6 activated carbon by supercritical methane as a probing molecule. The authors obtained the reliable PSD in the micropore range; however, the base of the local isotherms generated from GCMC captured the experimental pressure range lower than 3 MPa.

As mentioned by Do et al. there are a number of theoretical tools to study the problem of the supercritical fluid adsorption.[30] All of them are characterized by varying degrees of complexity. Among them, GCMC and nonlocal density functional theory (NDFT) give the most reliable picture of the supercritical fluid adsorption because both approaches are based on the statistical thermodynamics background.[39,40] Both of the advanced methods of adsorption phenomena modeling mentioned above can provide deep insights into the effects of pore structure on the adsorbed methane density. In the current study we selected the GCMC because it is well-known that NDFT cannot be used for the proper description of the fluid behavior in the very small nanopores due to the mean-field approximation.[41] GCMC is a statistical−mechanical method that rigorously solves a molecular-level model.[42] As there is no approximation in the solution of the statistical-mechanical model, accuracy of the GCMC simulation method depends only on the correct description of the fluid−fluid and fluid−solid interactions.[43,44] Because methane is a symmetrical molecule the GCMC protocol is reliable, simple, and powerful.[32]

In the current paper we investigate the basic features of methane adsorption both at an open graphite surface and in slitlike pores of different dimensions at 273 K applying the GCMC simulation. We adopted the experimental pressure range up to 16 MPa. In the next part of our study we present the model description (i.e., intermolecular potentials, the equations used for the evaluation of the surface excess isotherm, and the enthalpy of adsorption from GCMC simulation). Additionally, we present the model of the pore size analysis in the range of micropores. Further, a discussion of the results is presented in three subparts. The first one deals with the problem of the supercritical adsorption of methane at an open homogeneous graphite flat surface. In this part the solid−fluid interactions were adjusted on the basis of the experimental supercritical adsorption of methane on Graphon at 273 K.[30,51] With the knowledge of the realistic value of the solid−fluid interactions, the systematic investigation of adsorption in slitlike micropores is described. Finally, the reliable pore size analysis of the pure microporus pitch-based activated carbon fibers validates the current method.

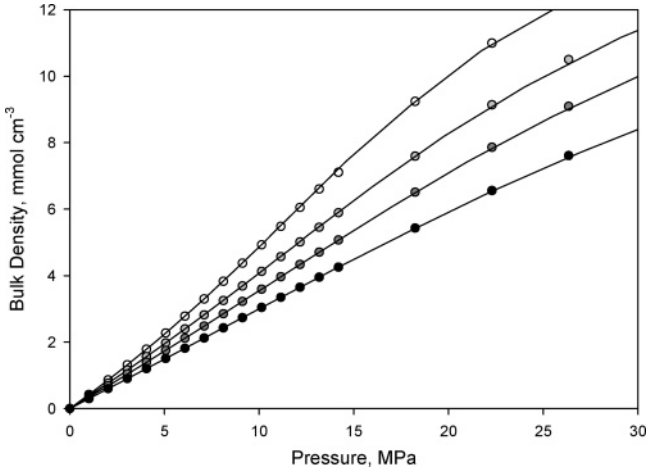

Figure 1. Comparison of the experimental equation of state for methane at $T = 294$, 328, 361, and 411 K (circles) with the ones obtained from Monte Carlo simulation in canonical ensemble (solid lines).

Description of the Model

In the simulation of supercritical methane adsorption in the slitlike micropores the grand canonical ensemble (i.e., fixed system volume V, temperature T, and chemical potential of the bulk fluid μ) was used.[39,42,43] All of the simulations were performed for a fluid in the slitlike micropores interacting via the truncated LJ pair potential,[42,43]

$$V_{ff}(r) = 4\epsilon_{ff}\left[\left(\frac{\sigma_{ff}}{r}\right)^{12} - \left(\frac{\sigma_{ff}}{r}\right)^{6}\right]\Theta(r_{cut} - r) \qquad (1)$$

Here, r is the distance between two interacting fluid molecules, σ_{ff} denotes the LJ fluid−fluid collision diameter, ϵ_{ff} is the LJ fluid−fluid potential well depth, $r_{cut} = 5\sigma_{ff}$ is the cutoff distance, and Θ denotes the Heaviside function. No long-range corrections were applied. LJ parameters $\sigma_{ff} = 0.381$ nm and $\epsilon_{ff}/k_b = 148.12$ K for methane interactions were taken from the work of the Cracknell and Nicholson.[45] The series of simulations in the canonical ensemble by the Windom's particle insertion method were carried out, to measure the excess part of the chemical potential and finally relate the total chemical potential of methane to its bulk density and pressure at desired temperatures (i.e., input parameters to GCMC).[39,42,46] All results obtained by applying Widom's particle insertion method were compared with phase diagrams of methane at a selected range of temperatures[47] to ensure the adequacy of the fluid−fluid interaction potential model (see Figure 1). Note that the simple one-center LJ fluid−fluid interaction potential describes the experimental data with very high precision and as a result validates the selected model of the fluid−fluid interaction (see Figure 1).

(37) Vishnyakov, A.; Piotrovskaya, E. M.; Brodskaya, E. N.; Votyakov, E. V.; Tovbin, Yu. K. *Langmuir* **2000**, *16*, 5955.
(38) Jiang, S. Y.; Rhykerd, C. L.; Gubbins, K. E. *Mol. Phys.* **1993**, *79*, 373.
(39) Frenkel, D.; Smith, B. *Understanding molecular simulation*; Academic Press: New York, 2002.
(40) Nicholson, D.; Parsonage, N. G. *Computer Simulation and Statistical Mechanics of Adsorption*; Academic Press: New York, 1977.
(41) Lastoskie, Ch.; Gubbins, K. E.; Quirke, N. *Langmuir* **1993**, *8*, 2693.
(42) Allen, M. P.; Tildesley, D. J. *Computer Simulation of Liquids*; Clarendon Press: Oxford, 1987.
(43) Gubbins, K. E., Quirke, N., Eds. *Molecular Simulation and Industrial Applications. Methods, Examples and Prospects*; Gordon and Breach Science Publishers: Singapore, 1996.
(44) Gelb, L. V.; Gubbins, K. E.; Radhakrishnan, R.; Sliwinska-Bartkowiak, M. *Rep. Prog. Phys.* **1999**, *62*, 1573.
(45) Cracknell, R. F.; Nicholson, D. *Adsorption* **1995**, *1*, 7.
(46) Widom, B. *J. Chem. Phys.* **1963**, *39*, 2808.
(47) Vagraftik, N. B. *The Handbook of Thermodynamic Properties of Gases and Liquids*; G.I.F.M.L.: Moscow, 1963 (in Russian).
(48) Kaneko, K.; Cracknell, R. F.; Nicholson, D. *Langmuir* **1994**, *10*, 4606.
(49) Gregg, S. J.; Sing, K. W. S. *Adsorption, Surface Area and Porosity*; Academic Press: London, 1982.
(50) Kowalczyk, P.; Tanaka, H.; Kanoh, H.; Kaneko, K. *Langmuir* **2004**, *42*, 1813.
(51) Findenegg, G. H.; Specovius, J. *Ber. Bunsen-Ges. Phys. Chem.* **1978**, 82, 174.

The interaction between a methane molecule and the plane graphite wall was modeled by the "10-4-3" potential derived by Steele,[43,44]

$$u_{sf}(z) = 2\pi\rho_s\epsilon_{sf}\sigma_{sf}^2\Delta\left[\frac{2}{5}\left(\frac{\sigma_{sf}}{z}\right)^{10} - \left(\frac{\sigma_{sf}}{z}\right)^4 - \left(\frac{\sigma_{sf}^4}{3\Delta(z+0.61\Delta)^3}\right)\right] \quad (2)$$

$$\epsilon_{sf} = (1-k_{sf})(\epsilon_{ff}\epsilon_{ss})^{1/2} \quad (3)$$

where Δ is the separation between the graphite layers (=0.335 nm), ρ_s is the number of carbon atoms per unit volume of graphite (=114 nm^{-3}), ϵ_{sf} and $\sigma_{sf} = (\sigma_{ff} + \sigma_{ss})/2$ (=0.3605 nm) are the solid−fluid potential parameters corresponding to the LJ model of molecular interactions, and z is the shortest distance between the fluid molecule and the plane passing through the centers of carbon atoms in the outermost layer. Although the Steele's potential neglects the lateral variation along the graphite plane (xy), it gives reasonable approximation of the real pore structure.[29] Moreover, the neglecting of the energetic inhomogeneity of the surface along the x and y directions is not expected to affect the results significantly at 273 K due to high kinetic energy of methane molecules. Because the Lorenz−Berthelot mixing rule is found to be inadequate in some cases, in the current paper the concept of the solid−fluid binary interaction parameter, k_{sf}, was used for adjusting ϵ_{sf} to the supercritical experimental data of methane on the primary flat surface of the homogeneous Graphon carbon black.[51,30] The approximation mentioned above is justified by the fact that the values for the LJ graphite−methane interactions usually used in simulations are the literature values rather than values derived from fitting the LJ parameters to methane adsorption on nonporous carbon black.

For a slitlike pore of width H, defined as the distance between the plane passing through all carbons atoms of the outmost layer of one wall and the corresponding plane of the opposite wall, the total solid−fluid interaction energy is given by[44,37]

$$V_{sf}(z) = u_{sf}(z) + u_{sf}(H-z) \quad (4)$$

Notice that the defined above pore width, H, should be corrected due to space inaccessible to fluid molecules (i.e., excluded volume). We avoid the method suggested by Aukett et al. who treated the space between "hard sphere" wall carbons atoms as the corrected/experimental pore width.[19] The error generated by this assumption increases as the pore width decreases. We use the following relation proposed by Kaneko et al.[48]

$$w_{eff} = H - 2z_0 + \sigma_{ff}, \quad z_0 = 0.8506\sigma_{sf} \quad (5)$$

Notice that eq 5 can be applied only for simple molecules interacting with the surface atoms by pure dispersion forces (i.e., argon, methane, carbon tetrachloride, etc.).

To compare with experiment, the simulated absolute values of adsorption should be converted to the excess quantity. Knowing the simulation pore geometry it can be simply done by the relation proposed by Matranga et al.,[25]

$$\Gamma(\rho_b) = N - V\rho_b \quad (6)$$

where V is the volume of the slitlike pore occupied by methane and ρ_b is the bulk density of the gaseous methane calculated by Widom's particle insertion method.[46]

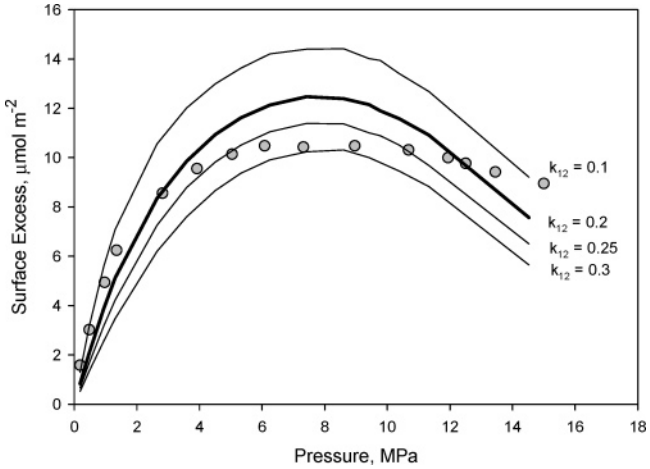

Figure 2. Fitting of the 273 K data of methane on Graphon carbon black with the solid−fluid binary interaction parameter as the fitting parameter. For all remaining GCMC simulations $k_{sf} = 0.2$ was selected (bold line).

To search for the PSD, we express the experimental excess of adsorption by the superposition of local excess isotherms calculated from the GCMC protocol,[49,55]

$$\Gamma(\rho_b) = \sum_j \Gamma_{loc}(\rho_b, w_{eff,j})\, f(w_{eff,j}) \quad (7)$$

where the $\Gamma_{loc}(\rho_b, w_{eff,j})$ is the Gibbs excess of adsorption in a slitlike micropore of effective width $w_{eff,j}$ at the pressure p, $\Gamma(\rho_b)$ denotes measured overall excess of adsorption, and $f(w_{eff,j})$ is the discreet analogue of the PSD function. Obviously, we assume both a non-negativity and a normalization constraint for the distribution function $f(w_{eff,j})$.[32,50,55]

Besides the surface excess of adsorption a thermodynamic quantity of interest that can be obtained form the GCMC is the isosteric enthalpy of adsorption. According to fluctuation theory, it is calculated from[40]

$$q_{iso} = \frac{\langle U\rangle\langle N\rangle - \langle UN\rangle}{\langle N^2\rangle - \langle N\rangle\langle N\rangle} + k_bT \quad (8)$$

where $\langle ...\rangle$ is the ensemble average, k_b is the Boltzmann constant, N denotes the number of particles, and U is the configuration energy of the system. This configuration energy can be divided into two contributions, one is due to the fluid−fluid interaction while the other is due to the fluid−solid interactions, that is, $U = U_{ff} + U_{sf}$. So finally the isosteric enthalpy of adsorption is given by[30,40]

$$q_{iso} = \left[\frac{\langle U_{ff}\rangle\langle N\rangle - \langle U_{ff}N\rangle}{\langle N^2\rangle - \langle N\rangle\langle N\rangle} + k_bT\right] + \frac{\langle U_{sf}\rangle\langle N\rangle - \langle U_{sf}\rangle\langle N\rangle}{\langle N^2\rangle - \langle N\rangle\langle N\rangle} \quad (9)$$

In the above equation the first term is the contribution from the fluid−fluid interaction and the molecular thermal energy, while the remaining term is the contribution form the solid−fluid interaction.

(52) Do, D. D.; Do, H. D. *Carbon* **2003**, *41*, 1777.
(53) Kowalczyk, P.; Kaneko, K.; Kanoh, H.; Tanaka, H.; Ustinov, E. A. *Abstract of Spring Meeting of Chemical Society of Japan* **2004**, *1*, 308.
(54) Tanaka, H.; El-Merraoui, M.; Steele, W. A.; Kaneko, K. *Phys. Chem. Lett.* **2002**, *352*, 334.
(55) Gauden, P. A.; Kowalczyk, P.; Terzyk, A. P. *Langmuir* **2003**, *19*, 4253.

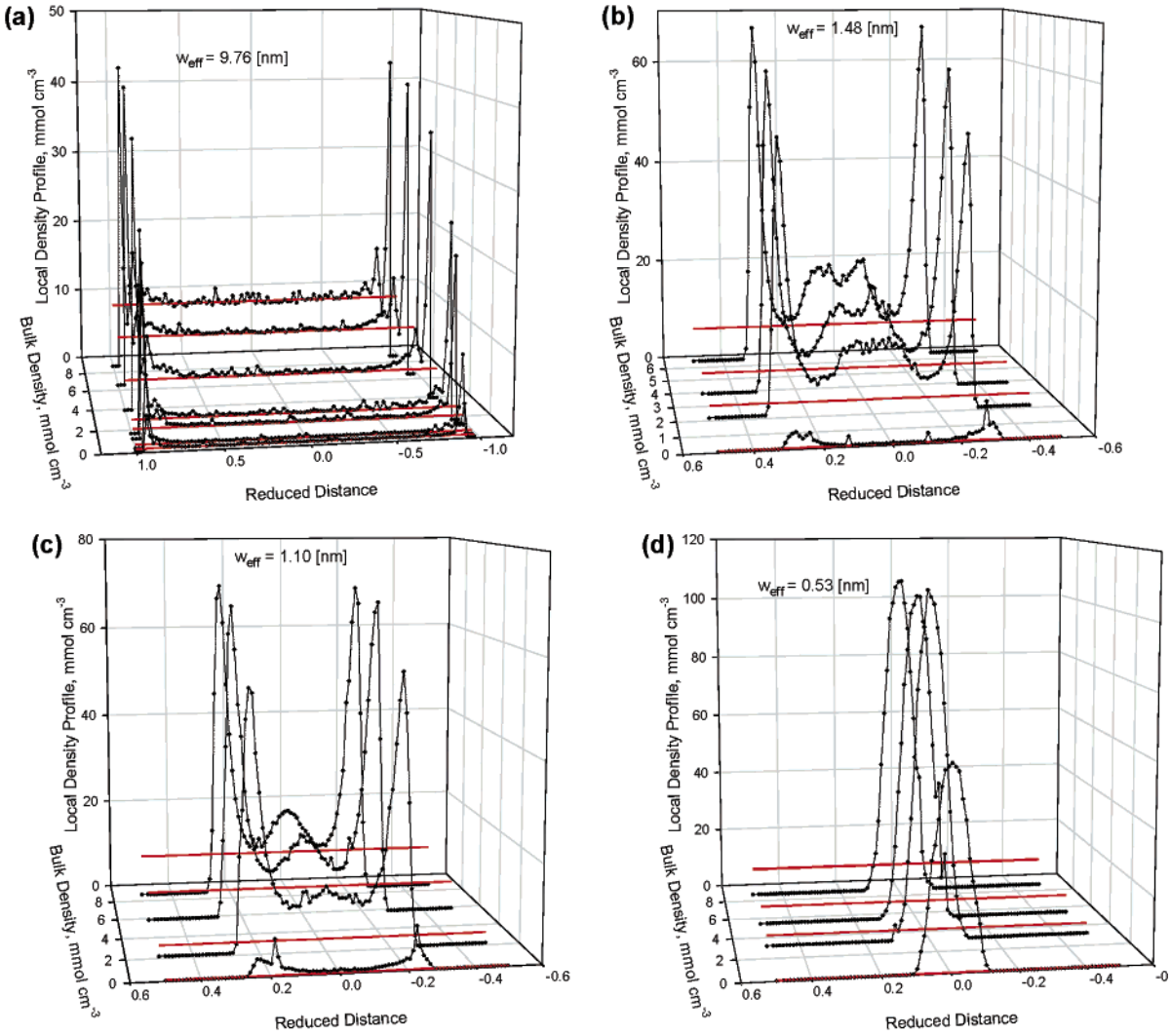

Figure 3. Local density profiles of methane at 273 K in slits of 9.76, 1.48, 1.10, and 0.53 nm. The interfaces are located at $z^* \equiv z\sigma_{ff}^{-1} = 1$ (−1). Horizontal solid red lines denote the bulk density corresponding to the displayed local density profiles.

In the current study, for every state and slitlike pore size, 7×10^7 GCMC configurations were generated. The first 2.5×10^7 configurations were discarded to guarantee equilibration, whereas the latter 4.5×10^7 configurations were used to average the desired thermodynamic properties. Additionally, in all simulations the local density profiles were collected during collection of the averages. For arbitrary selected points the fluctuations in total energy were stored and analyzed to ensure that the thermodynamic equilibrium was achieved. For the shorter Markov chains we observed high oscillations in the local density profiles.

Results and Discussion

Supercritical Adsorption of Methane at an Open Homogeneous Graphite Flat Surface. We applied the GCMC protocol to describe the adsorption of methane on the nonporous Graphon carbon black surface at 273 K. The methane data were taken from the Specovius and Findenegg study.[51] The only one parameter required for the prediction of the methane adsorption is the solid−fluid binary interaction parameter, k_{sf}, used for adjusting the LJ well depth for the solid−fluid interaction generated from the Lorenz−Berthelot mixing rule.

As one can see from Figure 2, GCMC qualitatively predicted the experimental surface excess of methane at 273 K. The quantitative differences are resulted from the simplicity of the model and the heterogeneity of studied carbon black.

To have insight into the supercritical methane behavior at an open homogeneous graphite flat surface, a series of the snapshots and local density profiles were collected (see Figure 3a). For the remaining GCMC simulation in slitlike pores of various sizes the value $k_{sf} = 0.2$ was selected as a representative. Notice that the Lorenz−Berthelot mixing rule overpredicted the solid−fluid interactions as in agreement with the earlier study of Do et al.[30] The good description of the experimental surface excess isotherm over the whole range of pressure is not possible due to many reasons, for example, the simplicity of the simulation model (i.e., perfect infinite homogeneous graphite structure, neglecting the influence of the solid surface into values of the LJ parameters, etc.). On the other hand, it should be noted that the surface excess is not a quantity that is directly measured experimentally, but rather it is calculated based on the assumption that we know accurately the true carbon density. The latter is usually obtained from the helium displacement method, and the validity of this method has been questioned in the literature. Therefore, if the incorrect value of the true carbon density is used the calculated surface excess is wrongly calculated. One thing is certain that the general picture of the GCMC predictions is physically corrected (see Figures 2 and 3). First of all the position of the surface

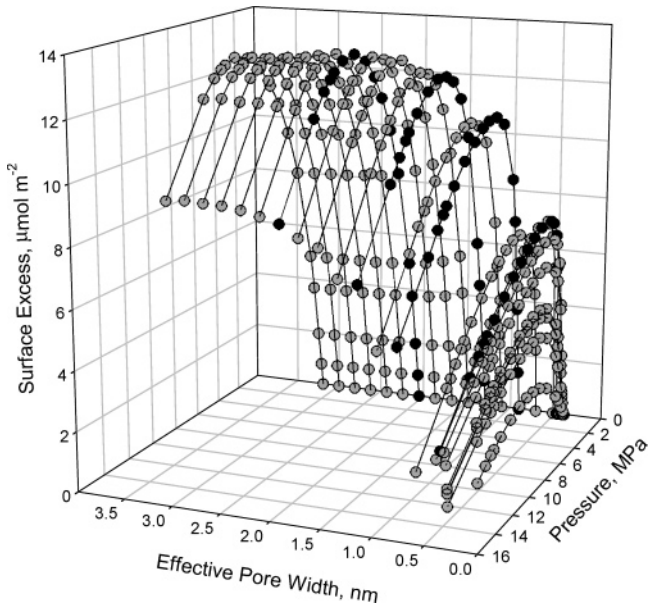

Figure 4. Methane surface excess adsorption isotherms simulated by the GCMC method in slit-shaped pores of various effective widths at 273 K. The selected reduced pores with $H^* = 1.9$, 3.0, 4.0, and 6.0 (from left to right) were marked by black circles.

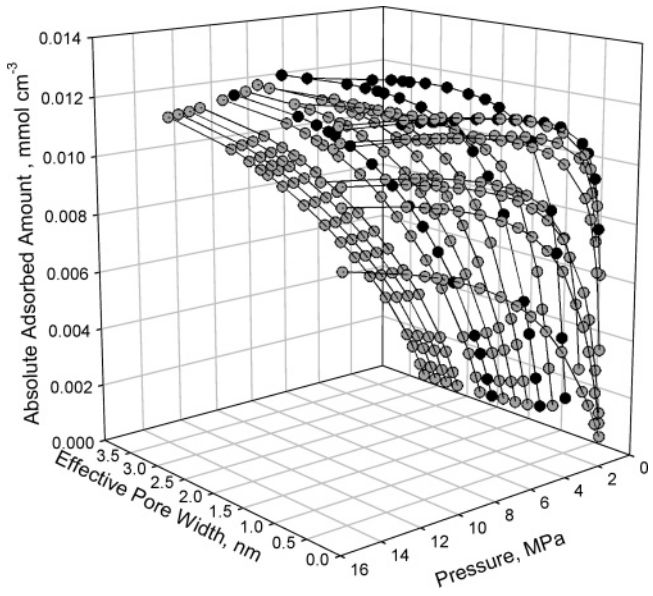

Figure 5. Methane absolute adsorbed isotherms simulated by the GCMC method in slit-shaped pores of various effective width at 273 K. Selected reduced pores with $H^* = 1.9$, 3.0, 4.0, and 6.0 (from left to right) were marked by black circles.

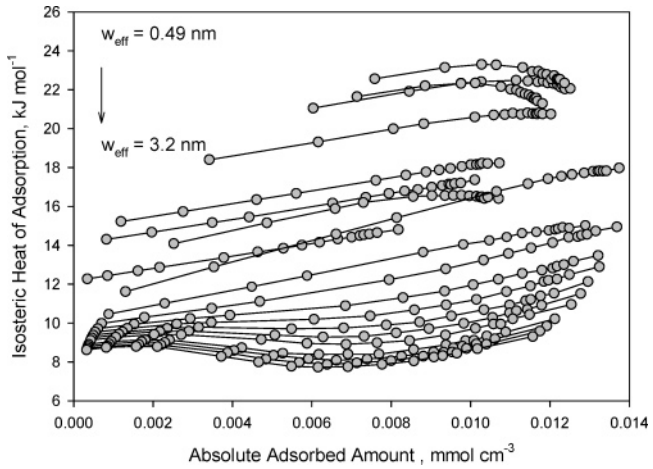

Figure 6. Isosteric enthalpy of adsorption simulated by the GCMC method in slit-shaped pores of various effective widths at 273 K.

excess maximum generated from the GCMC simulation with appropriative value of the solid−fluid binary interaction parameter is very close to experimental one. The flattering of the experimental maxima on the surface excess isotherm can be attributed to the heterogeneity of the Graphon carbon black (see Do and Do[52] and Kowalczyk et al.[53]). The local density profiles of methane are very close to that published by Ustinov et al.[31] and generally confirm the main densification of the supercritical fluid in the first and second layer near the structureless graphite surface (see Figure 3a). As one can suspect the adsorbed phase density in the central part of the pore is very close to the bulk phase density.

Supercritical Adsorption of Methane in Pores. Obviously, the key problem is getting insight into adsorption in pores of molecular sizes. The GCMC simulation is a common tool used for the investigation of the confined fluid properties.[30,32,37,44,45] Figure 4 presents the set of local excess isotherms of methane at 273 K obtained from the GCMC for a series of slitlike pores. As expected all computed adsorption isotherms are characterized by maxima and the pattern of shifting surface excess maxima with increasing pore size is clearly distinguished.[29] Qualitatively, this behavior is readily explained by the fact that the density near the graphite wall cannot increase indefinitely; hence, the surface excess decreases as the bulk density gradually approaches that near the graphite wall. The difference in the adsorption isotherms was associated with different packing structures of methane molecules (see Figures 3, 7, and 8). The methane molecules confined in the micropore tend to form an ordered structure favorable for both the molecule−surface and the intermolecular interactions. Unfilled voids in pores resulting in imperfect packing of methane lowered the value of the surface excess isotherm (see Figure 8). Beside this, it is clearly seen from Figures 3, 4, and 7 that the surface excess approaches a constant value when the pore size increases. Hence, if a pore is large enough it does not affect the adsorbed excess amount. As mentioned by Ustinov and Do,[31] this is the reason that in the range of pore sizes greater than approximately 2 nm the PSD function cannot be reliably determined from the supercritical isotherm data. All mentioned above features are clearly displayed in Figure 7. As one would expect, the dependence of the maximum surface excess and isosteric enthalpy of adsorption upon the effective pore size is not monotonic because of the packing effect, but rather they show oscillatory behavior. Clearly, the maximum corresponds to the pore where an additional layer can be accommodated within the pore; however, the oscillation of the maximum excess adsorbed amount versus effective pore width is a characteristic feature of the confined fluid in small pores. When pores become larger, such oscillation is rapidly diminishing (see Figure 7). It is worthwhile to point out that all features displayed in Figures 3, 4, and 7 are in agreement with the previous studies concerning supercritical methane adsorption in slightly different temperatures.[29,31] For example, according to Tanaka et al.[54] above the slitlike pore with $H = 6\sigma_{ff}$, the excess of adsorption does not change and, for the investigated temperature, that is, $T = 303$ K, this pore size corresponds to methane adsorption on the isolated open graphite layer. Moreover, Cracknell et al.[15] showed that at 274 K the optimal material for methane storage is a porous carbon

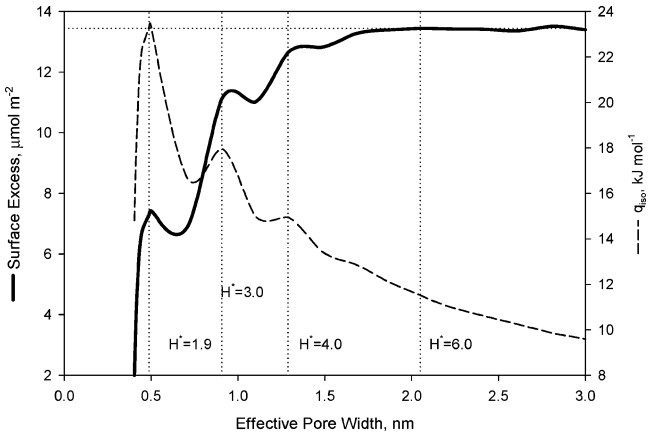

Figure 7. Effect of the effective pore width on the maximum surface excess and isosteric enthalpy of adsorption of methane adsorption at 273 K.

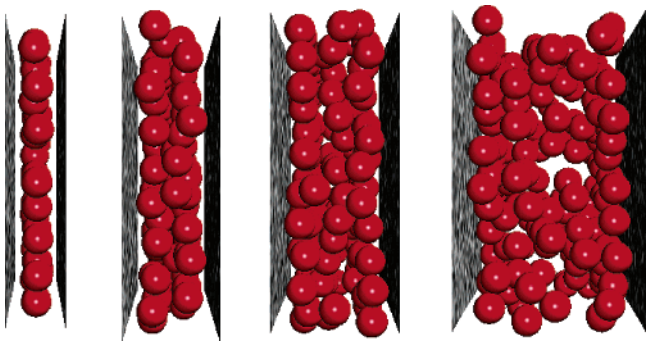

Figure 8. Snapshots of methane at maximum surface excess at 273 K for selected reduced pores with $H^* = 1.9$, 3.0, 4.0, and 6.0 (from left to right).

having a pore size large enough to contain two adsorbed layers of methane; however, they pointed out that at low pressures a pore of width $H = 2\sigma_{ff}$ would hold the most methane, while pores of width $H = 3\sigma_{ff}$ and $H = 4\sigma_{ff}$ would hold more at higher pressures (see Figures 4, 5, and 7). A similar conclusion can be found from the NDFT study of methane storage in the slitlike pore geometry by Tan and Gubbins.[29] They determined that an optimal carbon slit pore would have a width of 1.14 nm. Here, we want to point out that NDFT cannot be used for a qualitative prediction of the confined fluid properties in very dense systems due to mean field approximation. Consequently, computer simulations can only be applied for the proper modeling of the methane or hydrogen adsorption in ultrapores.[59,60] In Figure 5 the absolute adsorbed amount isotherms corresponding to the surface excess are displayed. As one can suspect the packing effect is mapped into the absolute value of adsorption in slitlike pores; however, this function is never decreasing. For the smallest pores the absolute value of adsorption (i.e., total storage value) tends to reach constant value in the considered adsorbate pressure range. Oppositely, for larger ones this function is increasing. It is clear because for larger pores the high packing and further compression of adsorbed molecules can be only achieved at higher pressures than those considered. In the considered adsorbate pressure range, the molecules in large pores tend to form clusters and the cluster size increases with pressure due to densification (see Figure 8). For the smallest perfect slitlike pores (i.e., pores that can accommodate an integral number of parallel layers) the adsorbed phase structure is highly ordered and the further increase in the absolute value of adsorption can be only achieved by molecule compression/rearrangement (see Figure 8). Consequently, in such a type of pores the absolute value of adsorption can achieve a plateau at a lower storage/pressure range. To fill the gap created by previous studies we computed the dependence of the isosteric enthalpy of adsorption (the enthalpy change on transferring a molecule from the gas phase to the adsorbed phase at constant temperature) upon loading (see Figure 6). Such a dependence is different from the one obtained for subcritical gas adsorption. Similarly, the very high values of enthalpy of adsorption in small pores come from overlapping of the forces generated by the opposite pore walls (i.e., enhancement in the solid−fluid potential energies). As one can see from Figure 6 the isosteric enthalpy of adsorption for the smallest pores is almost constant within the considered pressure range. For the intermediate pores with respect to loadings, the isosteric enthalpy of adsorption increases linearly. This increase is the result of increasing fluid−fluid interactions. Finally, for the largest considered pores the isosteric enthalpy of adsorption is characterized by smooth gradual changes resulting form the completion of the adsorbed layers. Oppositely to the variations of the enthalpy of adsorption versus loading at subcritical condition, the supercritical ones are characterized by regular smooth changes due to thermal motion and relatively weak fluid−fluid interaction of molecules (i.e., lack of condensation at adsorbed layers). It is worth pointing out that the estimated heat of adsorption is very close to the heat of adsorption at zero coverage reported by Cracknell et al.[15] It is primarily important to take the properties of the heat of adsorption into account for the storage problem during the projection of the vessel containing the methane as a fuel. As we demonstrate, GCMC simulation can be successfully applied for the determination of the energetic effect due to adsorption.

PSD from Supercritical Methane Adsorption. The PSD is the primary characteristic of the porous solid because of its influence on adsorption, diffusion, and so on. Figure 9 presents the PSDs of two microporous pitch-based activated carbon fibers, P5 and P20. The local surface excess isotherms of methane at 273 K generated from GCMC and well-documented ASA algorithm were used for the solution of the ill-posed problem without any prior assumption considering the PSD.[55,56] As mentioned by Aranovich and Donohue[57] and Ustinov and Do,[31] the PSD in the range of micropores, the total surface area, and other parameters characterizing the pore structure of the adsorbents calculated from the supercritical condition seems to be more realistic than those obtained from the subcritical one. Following this study we can concluded that the internal pore structures of both of the tested materials are considerably different. P5 ACF is characterized by a single exponential decreasing shape micropore size distribution with maxima around $w_{eff} = 0.45$ nm. On the other hand, a bimodal micropore size distribution is a characteristic feature of the P20 ACF. The appearance of the second peak on the micropore size distribution near $w_{eff} = 2.0$ can be confirmed by the drift of the surface

(56) Kowalczyk, P.; Gunko, V. M.; Terzyk, A. P.; Gauden, P. A.; Rong, H.; Ryu, Z.; Do, D. D. *Appl. Surf. Sci.* **2003**, *203*, 67.
(57) Aranovich, G. L.; Donohue, M. *J. Colloid Interface Sci.* **1996**, *180*, 537.
(58) Ohba, T.; Omori, T.; Kanoh, H.; Kaneko, K. *J. Phys. Chem. B* **2004**, *108*, 27.
(59) Lastoskie, C.; Quirke, N.; Gubbins, K. E. In *Equilibria and Dynamics of Gases Adsorption on Heterogeneous Solid Surfaces*; Rudzinski, W., Steele, W. A., Zgrablich, G., Eds.; Elsevier: Amsterdam, 1997; Vol. 104, p 745.
(60) Nguyen, T. X.; Bhatia, S. K.; Nicholson, D. *Langmuir* **2005**, *21*, 3187.

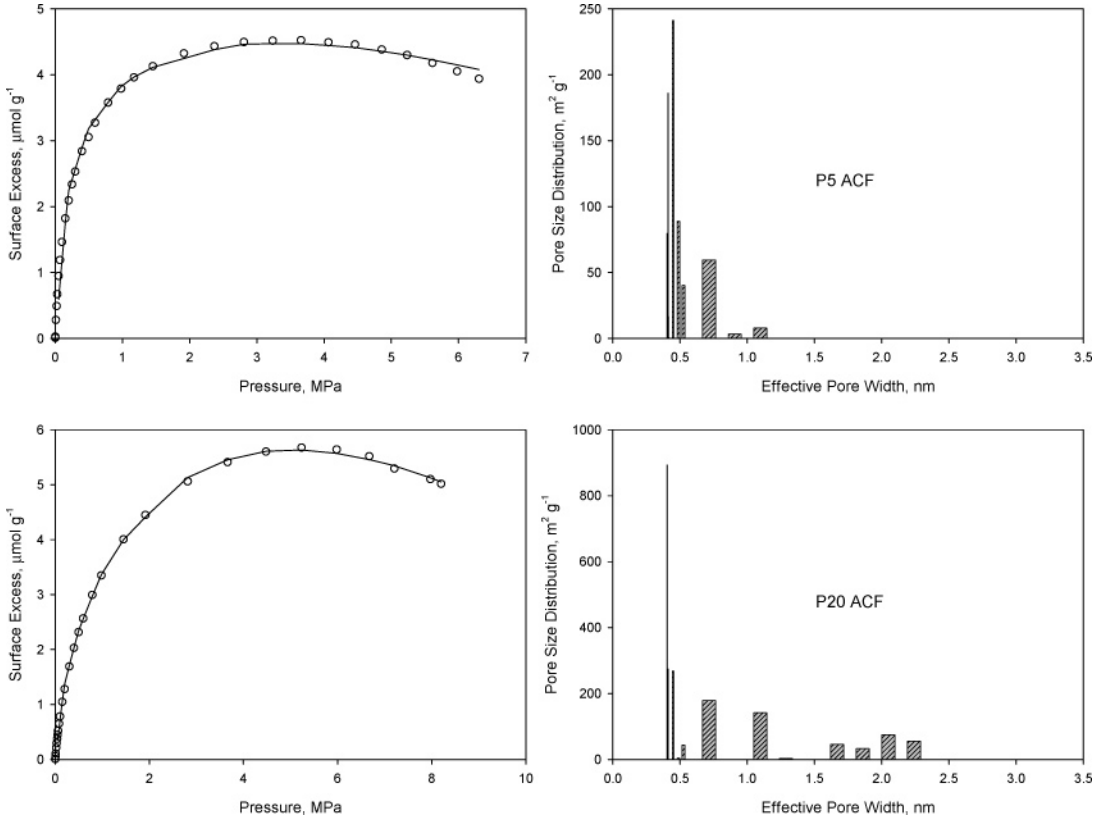

Figure 9. PSDs of P5 and P20 microporous pitch-based activated carbon fibers obtained by the GCMC with supercritical methane at 273 K.

excess maxima into higher values of pressure. As we show by GCMC simulations this feature is closely related to the increasing pore size (see Figure 4). For the case of P5 ACF the PSD obtained by Ohba et al. is very close to what we obtained in this paper.[58] On the contrary, for the P20 ACF the PSD obtained by Ohba et al. is quite different. It is very simple to explain if we take into account that these authors used very simple parametric fitting (one-modal Gaussian function) for the solution of the ill-posed problem.[50] Consequently, the calculated theoretical isotherm did not describe the experimental data properly in the whole range of the experimental pressures. Summing up, the nonparametric advanced numerical methods should be applied for the proper estimation of the PSD both from the subcritical and the supercritical adsorption data.[31,32,50,56] From the results of the present study one point is very important. It is worthy to underline that the PSD obtained from supercritical methane adsorption is not characterized by an artificial gap near $w_{\text{eff}} = 1.0$ frequently present in the PSDs evaluated from subcritical nitrogen isotherms. This fact favors the present methodology.

LA050126F